0026-895X/06/7001-143–153$20.00
MOLECULAR PHARMACOLOGY
Copyright © 2006 The American Society for Pharmacology and Experimental Therapeutics
Mol Pharmacol 70:143–153, 2006

Vol. 70, No. 1
23119/3122392
Printed in U.S.A.

Comparative Study of *ortho*- and *meta*-Nitrated Inhibitors of Catechol-*O*-methyltransferase: Interactions with the Active Site and Regioselectivity of *O*-Methylation

P. N. Palma, M. L. Rodrigues, M. Archer, M. J. Bonifácio, A. I. Loureiro, D. A. Learmonth, M. A. Carrondo, and P. Soares-da-Silva

Department of Research & Development, BIAL, S. Mamede do Coronado, Trofa, Portugal (P.N.P., M.J.B., A.I.L., D.A.L., P.S.-d.-S.); and Instituto de Tecnologia Química e Biológica (ITQB), Universidade Nova de Lisboa, Oeiras, Portugal (M.L.R., M.A., M.A.C.)

Received February 1, 2006; accepted April 17, 2006

ABSTRACT

In this work, we present a comparative case study of "*ortho*-" and "*meta*-nitrated" catecholic inhibitors of catechol-*O*-methyltransferase (COMT), with regard to their interaction with the catalytic site of the enzyme and the in vitro regioselective formation of their mono-*O*-methyl ether metabolites. In particular, the effects of altering the attachment position of the inhibitors' side-chain substituent, within the classic nitrocatechol pharmacophore, were investigated. For this purpose, we compared two simple regioisomeric nitrocatechol-type inhibitors of COMT, BIA 3-228 and BIA 8-176, which contain the benzoyl substituent attached at the *meta* and *ortho* positions, respectively, relative to the nitro group. The two compounds were slowly *O*-methylated by COMT in vitro, but the particular substitution pattern of each compound was shown to have a profound impact on the regioselectivity of their *O*-methylation. To provide a plausible interpretation of these results, a comprehensive analysis of the protein-inhibitor interactions and of the relative chemical susceptibility to *O*-methylation of the catechol hydroxyl groups was performed by means of docking simulations and ab initio molecular orbital calculations. The major structural and chemical factors that determine the enzyme regioselectivity of *O*-methylation were identified, and the X-ray structure of the complex of COMT with *S*-adenosyl-L-methionine and BIA 8-176 is herein disclosed. This is the first reported structure of the soluble form of COMT complexed with a nitrocatecholic inhibitor having a bulky substituent group in adjacent position (*ortho*) to the nitro group. Structural and dynamic aspects of this complex are analyzed and discussed, in the context of the present study.

Catechol-*O*-methyltransferase (COMT; EC 2.1.1.6) has received a great deal of attention during the last few decades because it is one of the enzymes that metabolizes L-DOPA, the principal drug currently used in the symptomatic treatment of patients afflicted with Parkinson's disease. Therefore, the clinical administration of effective COMT inhibitors, as adjuncts to L-DOPA, serves the purpose of reducing premature *O*-methylation of L-DOPA to 3-*O*-methyl-L-DOPA, thereby prolonging its half-life and increasing the amount of the drug gaining access to the brain (Männistö and Kaakkola, 1989, 1990; Bonifati and Meco, 1999).

Nitro-substituted catechol derivatives are typically potent reversible and competitive COMT inhibitors. Although these inhibitors possess the catechol binding motif common to COMT substrates, the presence of the strongly electron-withdrawing nitro substituent greatly reduces the extent of *O*-methylation of the catechol hydroxyl groups, making these compounds poor substrates for the enzyme (Bäckström et al., 1989; Borgulya et al., 1989). The crystallographic structures of the complexes between rat COMT and a few structurally different inhibitors have been published (Fig. 1). Since the appearance of the very first structure, showing COMT complexed with the small and clinically irrelevant inhibitor 3,5-dinitrocatechol (OR-486; Protein Data Bank code 1vid) (Vidgren et al., 1994), the enzyme has been successfully cocrystallized with a nonconventional bisubstrate inhibitor (Protein Data Bank code 1jr4) (Lerner et al., 2001) and, more recently, with the nitrocatecholic inhibitor BIA 3-335, pos-

This work was funded in part by Fundação para a Ciência e Technologia/AdI through research projects POCTI/COMT-HUM/2002 and POCTI/BME/38306/2001 and grant SFRH/BD/5228/2001 (to M.L.R.).
Article, publication date, and citation information can be found at http://molpharm.aspetjournals.org.
doi:10.1124/mol.106.023119.

ABBREVIATIONS: COMT, catechol-*O*-methyltransferase; S-COMT, soluble catechol-*O*-methyltransferase; SAM, *S*-adenosyl-L-methionine; BIA 3-228, 3,4-dihydroxy-5-nitrobenzophenone; BIA 8-176, 3,4-dihydroxy-2-nitrobenzophenone; MES, 2-(*N*-morpholino)ethanesulfonic acid; RMSd, root-mean-square deviation.

sessing a long side-chain substituent (1h1d) (Bonifácio et al., 2002; Learmonth et al., 2004).

The binding mode of the catechol moiety is highly conserved in all structures and is essentially constrained by the coordination of the hydroxyl oxygens to the magnesium ion and by the narrow boundaries of the entrance to the active site. However, depending on the nature of substituent(s), the catechol ring may be forced into one of two opposite orientations, thereby determining which of the two catechol hydroxyl groups (either the 3- or 4-hydroxyl) is exposed to the methyl donor cosubstrate. Catecholamines and many other catechol substrates have been shown to undergo preferential 3-*O*-methylation (Creveling et al., 1972; Thakker et al., 1986; Lotta et al., 1995), which can be explained in terms of the structure and interactions of the catechol ring substituents with the catalytic site residues (Lotta et al., 1995; Lau and Bruice, 1998; Palma et al., 2003). The regioselectivity of *O*-methylation, however, is not restricted to the substrates of COMT. Typical nitrocatecholic COMT inhibitors, although poor substrates of the enzyme, may also be partially *O*-methylated by COMT, originating mono-*O*-methyl ether derivatives (Da Prada et al., 1994; Dingemanse et al., 1996; Palma et al., 2003). Likewise, how does the structure of the inhibitor affect the regioselectivity of its enzymatically catalyzed *O*-methylation? In this work, we explore the effects of altering the relative position of a side chain substituent within the nitrocatechol ring on the molecular interactions of the inhibitor with the catalytic site of COMT and on the regioselectivity of its *O*-methylation. To the best of our knowledge, no other comparative or systematic studies have yet been published to address these aspects of the structure-activity relationships of COMT inhibitors.

For the present case study, we selected two relatively small regioisomeric COMT inhibitors, BIA 3-228 and BIA 8-176, described previously (Learmonth et al., 2002, 2005), that contain the nitrocatechol pharmacophore substituted with a benzoyl side chain (Fig. 2). They differ structurally in that BIA 3-228 contains the benzoyl fragment placed in the *meta* position relative to the nitro group, whereas in BIA 8-176, the side chain is at the "nonclassic" *ortho* position relative to the nitro group.

The above structural and biological parameters are herein studied by a combination of experimental and theoretical approaches and an interpretation of the results is attempted to identify the principal structural and chemical factors that determine the *O*-methylation regioselectivity with these compounds. In the course of this study, crystals of the recombinant rat S-COMT enzyme complexed with BIA 8-176 and SAM were successfully obtained (Rodrigues et al., 2005) and the X-ray structure, determined at 1.6 Å, is herein detailed. In fact, this constitutes the first report of the crystallographic structure of a complex between COMT and an *ortho*-nitrated catecholic inhibitor.

Materials and Methods

Chemicals

BIA 3-228, BIA 8-176, and the respective *O*-methylated derivatives of each were synthesized in the Laboratory of Chemistry (BIAL) according to methods described previously (Learmonth and Freitas, 2002; Learmonth et al., 2002, 2005).

In Vitro *O*-Methylation Assays

Rat liver S-COMT was prepared as described previously (Bonifacio et al., 2003). The *O*-methylation of BIA 3-228 or BIA 8-176 was evaluated by incubating a 10 μM concentration of the compound with rat S-COMT (1 mg/ml total protein) at 37°C in the presence of 500 μM SAM, 100 μM $MgCl_2$, and 1 mM EGTA in 5 mM sodium phosphate buffer at pH 7.8. Reactions were terminated with 1% formic acid in acetonitrile and reaction products were analyzed by liquid chromatography/atmospheric pressure electrospray ionization mass spectrometry (HP 1100 Series; Agilent Technologies, Palo Alto, CA) with negative ion detection. Resolution was performed on a Lichrospher 100 RP-18 column (LiChroCART 250-3; 5 μm; Merck, Darmstadt, Germany). The mobile phases used were as follows: mobile phase A: water and 1% formic acid (v/v); mobile phase B, acetonitrile and 1% formic acid (v/v). The gradient conditions at 0 min were 50% of A and 50% of B and, at 10 min, 45% A and 55% B. The flow rate was 0.5 ml/min, the injection volume was 20 μl, and the stop time was 15 min. Selected ion monitoring, with detection set for the molecular ion of each compound of interest, was used for quantification. The analytical range used extended from 10 ng/ml to 500 ng/ml for the standards of the monomethyl ether derivatives of BIA 3-228 and BIA 8-176.

Crystal Structure Determination

The crystallization and X-ray diffraction data collection of S-COMT/SAM/BIA 8-176 complex has been described in detail elsewhere (Rodrigues et al., 2005). In summary, the complex was crystallized in 8% polyethylene glycol 6K and 0.1 M MES at pH 6.0, using rat S-COMT expressed in *Escherichia coli*. Diffraction data were collected until 1.6 Å, at a synchrotron radiation source. Crystals of S-COMT in complex with BIA 8-176 belong to the monoclinic space group $P2_1$ (a = 52.77 Å, b = 79.63 Å, c = 61.54 Å, and β = 91.14°) and contain two molecules in the asymmetric unit. The three-dimensional structure was determined by the molecular replacement method, using protein coordinates from the S-

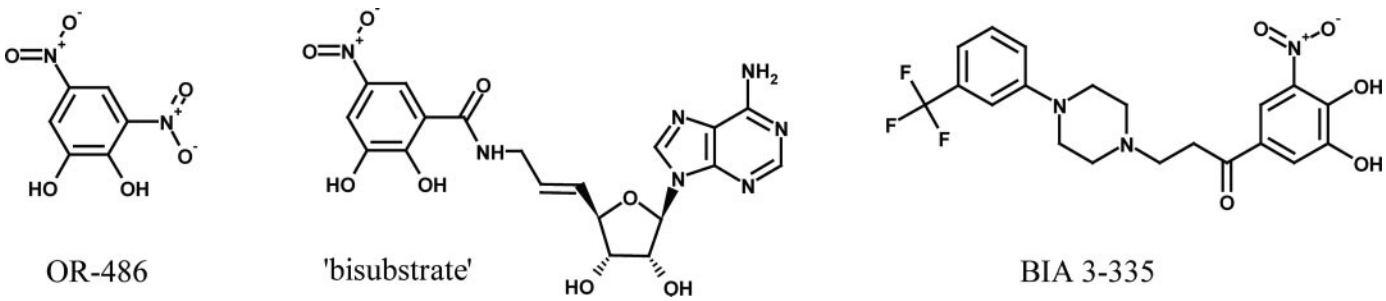

Fig. 1. Structures of inhibitors of catechol-*O*-methyltransferase that have been successfully cocrystallized with the enzyme.

COMT/SAM/BIA 3-335 complex crystal structure (Protein Data Bank code 1H1D) (Bonifácio et al., 2002). Model building and refinement was carried out using ARP/wARP and refmac programs from the CCP4 suite (Collaborative Computational Project, Number 4). TURBO graphical interface (Roussel and Cambilau, 1989) was used to fit the model into the electron density maps. The final refined model shows R_{factor} and R_{free} of 14.9 and 17.8%, respectively.

Computational Methods

Molecular Docking. The atomic coordinates of rat S-COMT were obtained from the crystal structure reported herein, after removal of the cocrystallized inhibitor, of all water molecules except HOH400 coordinated to Mg^{2+} and of any additional solvent molecules. The crystal asymmetric unit comprises two COMT complexes whose atomic coordinates are nearly identical (RMSd between the two complexes is 0.78 Å considering every nonhydrogen atom and 0.18 Å for all atoms including only the bound inhibitor and residues within a 5-Å radius from it). Therefore, for practical reasons, coordinates from only one monomer (monomer A) were used in all studies that involve the physiological form of COMT. All hydrogen atoms were added to the protein using standard procedures and considering amino acid residues in their typical physiological ionization forms. Flexible docking between COMT and the inhibitor was performed with the genetic algorithm GOLD ver.2.2 (Jones et al., 1995a,b, 1997; Nissink et al., 2002; Verdonk et al., 2003) (CCDC, Cambridge, UK). The exploration of the conformational space was done from a population of 100 individual conformations subjected to 100,000 mutational generations using a selection pressure of 1.1. All atoms at the COMT molecular surface within a radius of 14.0 Å from the Mg^{2+} ion were used as the target binding site. The coordination of the catechol hydroxyl groups to the Mg^{2+} ion is treated within GOLD force field as a donor-acceptor type of bond.

Docking was performed so as to generate models of the purportedly "activated" enzyme-inhibitor complex, where the proton of one of the catechol hydroxyls is transferred to the vicinal basic NH_2 of Lys144 side chain (Zheng and Bruice, 1997; Lau and Bruice, 1998; Kuhn and Kollman, 2000). The ε-amino group of the catalytic Lys144 was therefore modeled in the protonated state, whereas the catecholic ligand was docked in the mono-ionized form. To sample both *ortho* and *meta* poses and to compare the corresponding binding energetics, two independent sets of docking experiments were performed using distance constraints to bias the orientation of the nitrocatechol moiety within the active site. The ionized hydroxyl was always preset to be in the proximity of the positively charged ε-amine of Lys144 and methylsulfonium of SAM. These constraints, however, did not hamper the full flexible structure optimization of the ligand in each pose. Furthermore, given the nondeterministic nature of genetic algorithms, 20 independent docking runs were performed for each configuration, starting from random conformations and orientations of the ligands. The full set of docked structures was then analyzed as an ensemble of alternative complexes. Finally, all docked structures (protein and inhibitor) were energy-minimized to relieve any strains between the ligand and the protein and to mimic the "induced fit" between the two molecules. The MMFF94 force field (Halgren, 1996, 1999) was used with the molecular modeling package SYBYL (Tripos Inc., St. Louis, MO).

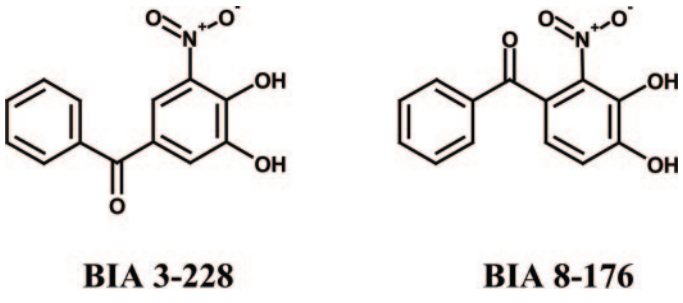

Fig. 2. Regioisomeric COMT inhibitors BIA 3-228 and BIA 8-176.

Hydrophatic Interactions. The protein-ligand interactions were evaluated using the empirically based HINT (Hydrophatic Interactions) potential function (Kellogg et al., 1992), as implemented in SYBYL. Partitioning of the apoprotein was done using the dictionary method and inferring the ionization states of protein residues from their explicit hydrogen count. For the cosubstrate (SAM) and the inhibitor, partitioning was calculated explicitly and by applying corrective factors to polar proximity effects using the via-bond method. Polar interactions were directed along vectors, coinciding with lone pairs or π orbitals. HINT cannot evaluate interactions with metals; therefore, the magnesium ion as well as the coordinated water molecule was neglected. HINT score assigns positive values to stabilizing energies and negative values otherwise. Stabilizing contributions to the HINT scores include acid-base, hydrophobic-hydrophobic interactions and hydrogen bonds, whereas unfavorable contributions include acid-acid, base-base, and hydrophobic-polar interactions.

Molecular Orbital Calculations. Molecular orbital calculations were computed using MOPAC2002 v.2.5.0 (Fujitsu Limited, Tokyo, Japan). Structures were prepared in the following way. To include the effects of the surrounding active site in the molecular orbital calculations, the structures BIA 3-228 and BIA 8-176 (as well as those of reference molecules catechol and 3,5-dinitrocatechol) in complex with COMT were taken from the refined lowest-energy docked poses obtained as described above. To keep the system amenable to molecular orbital calculations, the active site was simplified by retaining only the relevant atoms (i.e., the magnesium ion; its ligands Asp141, Asp169, Asn170; and the coordinated water molecule). The ligand-interacting residues Glu199 and Lys144 and the "gatekeeper" residues Trp38, Met40, Trp143, Pro174, and Leu198 were also retained to provide hydrogen bonding to the ligand and to constrain its optimization on site. The SAM methyl donor was modeled by a small $S^+(CH_3)_3$ molecule and the residues above were truncated at appropriated sp^3 carbons of their side chains, to further reduce the number of atomic centers. The structure of the ligands was finally optimized within the constrained active site coordinates using the MOPAC PM5 semiempirical Hamiltonian, with the program CAChe WS Pro v.6.1.10 (Fujitsu Limited). Finally, the electrophilic superdelocalizability $S_r(E)$ indices were computed from the molecular orbitals, at the ionized catecholate oxygen atom, near Lys144 and $S^+(CH_3)_3$. A fixed (acceptor) reagent energy of -3 eV was used.

Results

The purpose of this section is to evaluate the effects of altering the position of the benzoyl substituent from the *meta* to the *ortho* position, relative to the nitro group, on the molecular interactions of the inhibitors BIA 3-228 and BIA 8-176 with the catalytic site of COMT and the resulting regioselectivity of *O*-methylation.

To facilitate comparison of the sites of *O*-methylation within *meta*-nitrated and *ortho*-nitrated catecholic inhibitors, a nomenclature focused on the nitrocatechol structure will be used throughout the remaining text, instead of standard systematic atom numbering. Therefore, the catechol hydroxyl groups will be denominated according to their positions relative to the nitro group. The hydroxyl located in *meta position*, relative to the nitro group, will be noted herein as *meta*-hydroxyl, whereas the other hydroxyl function, *ortho* to the nitro group, will be identified as *ortho*-hydroxyl. Therefore, the two hypothetical bound orientations of the nitrocatechol moiety, will be denoted as *ortho* or *meta* configurations (or poses), reflecting which of the two hydroxyls is accessible

to the methylsulfonium. These two alternative configurations are illustrated in Fig. 3, with BIA 8-176.

In Vitro Assessment of *O*-Methylation Regioselectivity

BIA 3-228 and BIA 8-176 each originated two mono-*O*-methyl ether metabolites in a time-dependent manner (Fig. 4), when incubated with rat liver S-COMT supplemented with SAM and $MgCl_2$ as detailed under *Materials and Methods*.

Although relatively small amounts of the methylated metabolites were formed (up to 11% of the administered substrate was methylated after a long incubation period of 120 min with the enzyme), the regioselectivity of *O*-methylation was clearly distinct for the two compounds. The fraction of BIA 3-228 converted to its *meta*-*O*-methyl derivative after 120 min of incubation was only approximately 4.6%, yet this was still twice the fraction of the regioisomeric *ortho*-*O*-methylated product formed (2.2%). This contrasts with the results obtained for BIA 8-176, which is found to be preferentially *O*-methylated at the *ortho*-hydroxyl oxygen. Moreover, *O*-methylation of BIA 8-176 is more regioselective, with the ratio of *ortho*-/*meta*-*O*-methylated products being approximately 7.5. In addition, the *ortho*-*O*-methylation of BIA 8-176 is more extensive than that of BIA 3-228, whereas the opposite is true for the *O*-methylation at the *meta*-hydroxyl position.

Molecular Modeling of Enzyme Binding and *O*-Methylation Reactions

The experimental determination of the preferred site of *O*-methylation of compounds BIA 3-228 and BIA 8-176 may provide a first indirect information on how the two molecules interact with the catalytic site. However, the observed regioselectivity is also likely to depend on the relative propensities of each of the two catechol hydroxyls to accept a methyl group from SAM, within the framework of the catalytic site. To interpret the observed regioselectivities at the molecular level, contributions from those two distinct determinants must be estimated and balanced.

Docking Simulations. The configurational space of interaction of BIA 3-228 and BIA 8-176 within the active site of COMT (physiological monomeric form), was explored using molecular docking simulations followed by full energy optimization of the hypothetical complexes and by hydrophatic interactions evaluation, as detailed under *Materials and Methods*. The final docking results are illustrated in Fig. 5, which represents all docked structures of the two inhibitors, obtained in *ortho* and *meta* configurations.

The docked structures show extremely conserved atomic positions of the optimized catechol moiety, at the active site. Both hydroxyls coordinate the magnesium ion (average Mg-O distance = 2.19 ± 0.02 Å) and form hydrogen bonds with Glu199 and Lys144. The nitrocatechol moiety is constrained within the boundaries of the active site pocked, flanked by the hydrophobic residues Trp38, Pro174, Trp143, and Leu198. Moreover, it can hypothetically fit into either *meta* or *ortho* orientations. The benzoyl side chain, on the other hand, extends out of the catalytic pocket, toward the solvent. Despite the small size and limited flexibility of this short substituent, its conformation is also relatively constrained by the protein surroundings.

It is noted that the nitro group of BIA 8-176 adopts different torsion angles, out of the plane of the catechol ring, that are correlated with the conformations of the benzoyl substituent (Fig. 5, C and D). Indeed, there are intramolecular steric clashes between the atoms of the nitro group and the vicinal carbonyl function of the side chain, which prevent the two groups to align in the plane of the catechol ring.

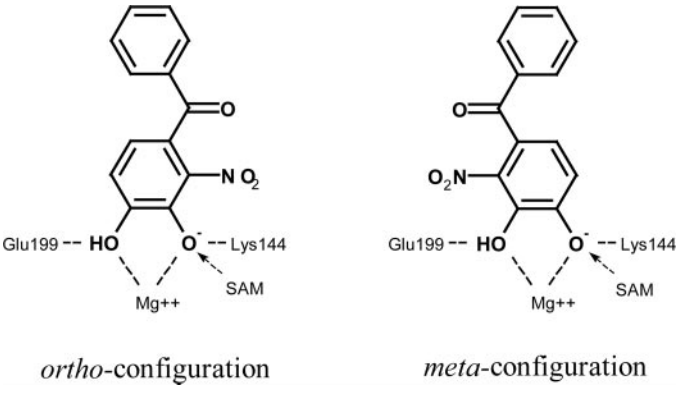

Fig. 3. Schematic representation of two hypothetical bound configurations of nitrocatecholic COMT inhibitors. In the *ortho* configuration, the nitro group is oriented toward SAM, whereas in the *meta* configuration, the nitrocatechol fragment is rotated 180° about the symmetry axis of the catechol ring. The two binding alternatives are illustrated with the structure of BIA 8-176.

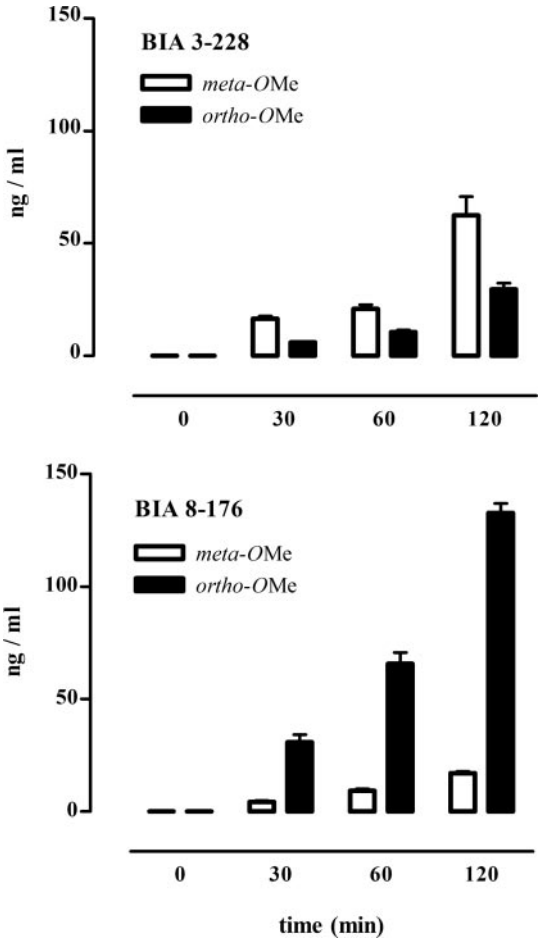

Fig. 4. Regioselectivity of *O*-methylation of COMT inhibitors. Concentrations of *O*-methyl ether derivatives formed from BIA 3-228 (left) or BIA 8-176 (right) at various time intervals. In each plot, the white and the dark bars represent the *meta*- and *ortho*-*O*-methylated metabolites, respectively. Error bars represent S.E.M. of $n = 3$.

The energetics of the protein-ligand interactions was evaluated by scoring every docked pose of BIA 3-228 and BIA 8-176, using the HINT potential, has described. Figure 6 plots the HINT intermolecular interaction scores of every docked ligand, against the RMSd between the heavy atoms of the corresponding structures and those of the highest scoring (lowest energy) pose of each compound.

Note that the interaction terms involving the magnesium ion and the ligand were neglected in our current analysis, given that metal interactions are not parameterized within HINT potential functions. However, the geometry of the Mg-O coordination bonds is highly conserved in every docked pose. Therefore, the neglect of such nearly invariable terms should still be a valid approximation for comparing different docked configurations.

The first and most relevant observation is that for either of the two inhibitors, BIA 3-228 or BIA 8-176, the formation of hypothetical complexes with COMT in the *ortho* configuration (Fig. 6, circles) is predicted to be thermodynamically more favorable (higher HINT scores) than in *meta* configurations (Fig. 6, triangles). Moreover, the average energy (score) separation between the two opposite configurations is approximately 1.6 times greater for BIA 8-176 than it is for BIA 3-228. A closer analysis of the interaction energetics reveals that the greater relative stability of the *ortho* configurations can be mainly attributed to the positioning and interactions of the nitro group and, to a lesser extent, to that of the benzoyl side chain. When binding in a *meta* configuration, the nitro group is forced into sterically conflicting interactions against the hydrophobic side chain of Leu198, which induces penalizing conformational changes. Moreover, the electron-rich NO_2 group is strongly destabilized in that position because of repulsive electrostatic interactions with the negatively charged Glu199 (Fig. 5, B and D). Conversely, in the *ortho* configuration, the nitro group fits nicely within the catalytic pocket, establishing favorable van der Waals interactions with the indole ring system of Trp143 (Fig. 5, A and C). In addition, the neighboring positive charges of the acidic ε-amine of Lys144 and the methylsulfonium of SAM also contribute to stabilizing the electronegative nitro group in that pose.

In contrast, the benzoyl substituent can be accommodated at either side of the catalytic pocket with only moderate disturbance of the complex stability. Nevertheless, differences are mostly due to uncompensated interactions between the polar carbonyl group of the substituent and the hydrophobic Pro174 in certain orientations of the inhibitor (Fig. 5, A and D). The benzoyl side chain contributes to favoring those complex configurations where it is facing the edge of the catalytic pocket flanked by Trp143 and Met40 (Fig. 5, B and C), as opposed to the Leu198 side (Fig. 5, A and D). Therefore, in the case of BIA 8-176, both the benzoyl side chain and the nitro group concurrently contribute to reinforce the thermodynamic stabilization of the *ortho* complexes relative to *meta* bound configurations. Conversely, in the case of BIA 3-228, the two catechol substituents act in opposite directions with respect to favoring one or the other pose, therefore attenuating the energy gap between the two types of complexes (Fig. 6).

In summary, BIA 3-228 and BIA 8-176 are predicted to bind to COMT preferentially in the *ortho* configuration, and this binding selectivity is mainly determined by steric and electrostatic interactions of the nitro group within the active site. In addition, the position of attachment of the benzoyl

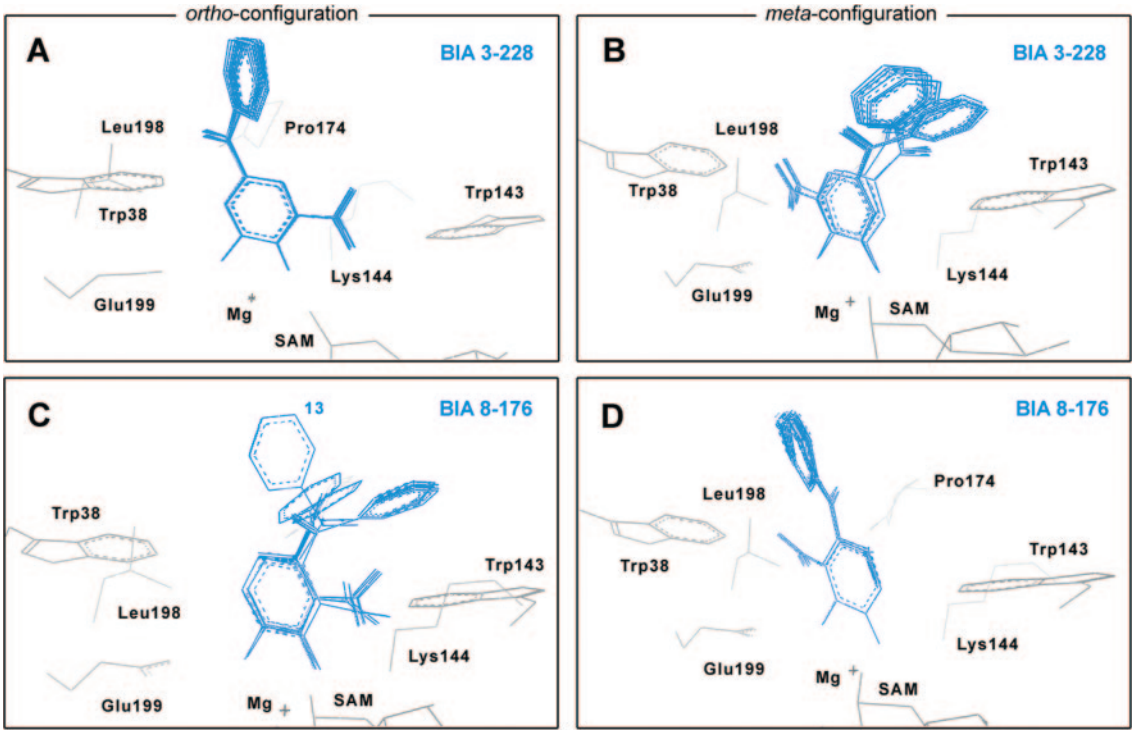

Fig. 5. Docking results of COMT with the regioisomeric inhibitors BIA 3-228 and BIA 8-176. Each panel represents twenty independently docked poses, generated in one of the two hypothetical configurations. A and C, *ortho* configuration; B and D, *meta* configuration. The amino acid side chains of residues comprising the active site are shown in gray and BIA 8-176 is represented in blue. The individual docked structure #13 is identified (see text).

substituent to nitrocatechol fragment of the inhibitors should affect, to a limited extent, the resulting ratio of populations of complexes in *ortho* and *meta* configurations. For BIA 8-176, that ratio is expected to be higher, on the basis of the current docking analysis.

Theoretical Analysis of Chemical Reactivity. The catalytic and inhibition mechanisms of COMT have been studied extensively by structural and theoretical methods (Vidgren and Ovaska, 1997; Zheng and Bruice, 1997; Lau and Bruice, 1998; Kahn and Bruice, 2000; Kuhn and Kollman, 2000; Lautala et al., 2001; Sipila and Taskinen, 2004; Chen et al., 2005). The catalytic process is initiated by the proton transfer from one of the catechol hydroxyls to the purportedly basic ε-amino group of Lys144. Once ionized, the nucleophilic hydroxylate oxygen may attack the electron-deficient methylsulfonium group of SAM leading to a methyl transfer proceeding by a S_N2-type reaction.

The chemical reactivity of charge transfer processes in conjugated systems may be estimated by means of dynamic reactivity indices derived from molecular orbital theory. In particular, the computed electrophilic superdelocalizability, $S_r(E)$, on an atom r can be related to the contribution made by that atom to the formation of a charge-transfer complex with a second, electrophilic reagent (Fukui et al., 1954, 1957; Karelson and Lobanov, 1996). The superdelocalizability indices can be employed to compare the reactivities of different atoms within a given molecule or between corresponding atoms in different molecules. In the particular case of the catecholic ligands (substrates or inhibitors), the greater the electrophilic superdelocalizability of the ionized hydroxylate oxygen, the more likely that oxygen is to be methylated, provided that it is accessible to the electrophilic methyl donor, in adequate reactive geometry. On the contrary, a lower value of $S_r(E)$ indicates a relatively unreactive atom with the electrophilic reactant.

The reactivity indices were computed for BIA 3-228 and BIA 8-176 considering each of the two possible modes of binding. The effects of the active site environment (i.e., the magnesium ion, the positively charged methylsulfonium of SAM, and the catalytic residues) were taken into account by considering those atoms in the molecular orbital calculations. The bound geometries of the ligands, as well as of the enzyme active site, were taken from the refined lowest-energy docked poses and truncated, as described under *Materials and Methods*. The catechol hydroxyl oxygen near Lys144 and the methylsulfonium was modeled in the ionized form (keeping the other hydroxyl protonated), and the structure of the complex model was optimized with MOPAC and the PM5 Hamiltonian, keeping the protein atoms constrained (except Glu199, Lys144, Mg^{2+}, and the methylsulfonium). The electrophilic superdelocalizability indices were finally computed from the molecular orbitals over the ionized catechol hydroxylate oxygen. For comparison, the values of *S*r(E) were also computed in the same way for the reactive nonsubstituted catechol (positive control) and of the doubly substituted 3,5-dinitrocatechol. Results are plotted in Fig. 7.

A practical relative scale of reactivities can be circumscribed by the superdelocalizability indices of the nonsubstituted catechol (which is easily *O*-methylated) and of 3,5-dinitrocatechol, which is doubly substituted with a strong electron-withdrawing group. As expected, these results indicate that the electron delocalization potentials of the nitro and benzoyl substituents induce a marked decrease in the electrophilic superdelocalizability of the hydroxylate oxygens (hence of their nucleophilicity and reactivity), compared with those of the unsubstituted catechol ring. Moreover, the strongly electron-withdrawing nitro group exerts a dominant effect on lowering the nucleophilicity of the hydroxylate oxygens. In these structures, the *ortho*-hydroxyl oxygen is indicated to be the least reactive of the two nitrocatechol hydroxyls. A comparison of the results with superdelocalizability indices computed for the isolated molecules (results not shown) indicates that the catalytic environment provided by the enzyme generally increases the *S*r(E) of the ligand's reactive oxygen, hence assisting its reactivity. However, it does not significantly affect the relations plotted in Fig. 7.

Moreover, the difference of reactivities between the two

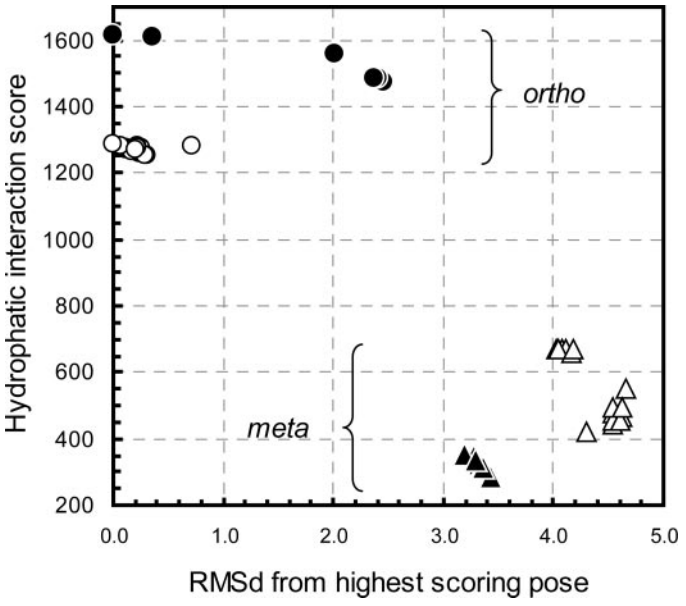

Fig. 6. Hydrophatic interaction scores of every docked structure, calculated with the HINT potential. White markings represent the docked poses of BIA 3-228 and black symbols those of BIA 8-176. In addition, circles represent molecules docked in *ortho* configuration, whereas *meta* poses are represented by triangles. The abscissa represents the RMSd between the atomic coordinates (heavy atoms) of each docked structure and those of the highest scoring pose of each compound. Higher HINT scores indicate more stable complexes.

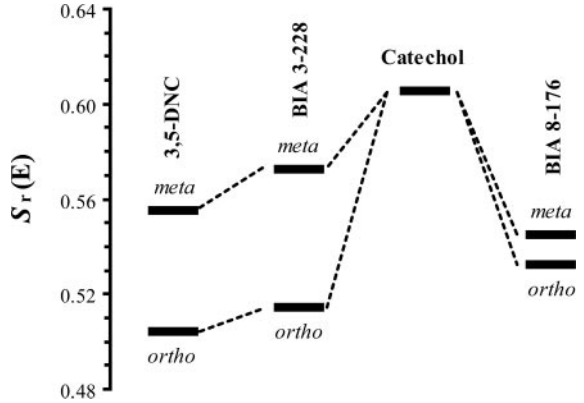

Fig. 7. Electrophilic superdelocalizability indices, *S*r(E), computed on each of the ionized catecholate oxygens (*ortho* or *meta* relative to nitro), while keeping the other hydroxyl protonated. See text for details of calculation.

catechol hydroxyls strongly depends on the relative position of the benzoyl side chain within the nitrocatechol moiety. The attachment of the benzoyl substituent in *meta* position, relative to the nitro group, as in BIA 3-228, induces a larger separation of the superdelocalizability indices of the two hydroxylates, whereas the alternative position of the benzoyl side chain, *ortho* to the nitro substituent as in BIA 8-176, results in a great reduction of the difference between the *S*r(E) values of the two catechol hydroxylates.

Based solely on the relative chemical reactivities of the "activated" hydroxyl oxygens within the active site, one would conclude that the complexes with the nitrocatecholic inhibitors in ortho configuration are generally less reactive than those complexes formed in the alternative orientation. In this case, the *ortho*-hydroxyl oxygen of BIA 8-176 could be slightly more reactive than the equivalent oxygen of BIA 3-228. On the other hand, of those complexes that form in *meta* configuration, one would expect that BIA 3-228 would be *meta*-*O*-methylated at a higher rate than BIA 8-176. These data are complementary to the docking results presented above, and together they provide a plausible reasoning for the observed regioselectivity of *O*-methylation, as detailed in the discussion section.

Crystal Structure of S-COMT in Complex with BIA 8-176

Tentative efforts to cocrystallize S-COMT with several different inhibitors led to the successful structure determination of S-COMT, complexed with SAM and the recently described *ortho*-nitrated inhibitor BIA 8-176.

General Structure Description. The ternary complex S-COMT/SAM/BIA8-176 crystallized in a monoclinic space group ($P2_1$), with two protein molecules in the asymmetric unit. This contrasts with previously reported S-COMT complexes (Vidgren et al., 1994; Lerner et al., 2001; Bonifácio et al., 2002), which crystallized in the trigonal space group $P3_221$, containing only one protein molecule per asymmetric unit. The refined model comprises 214 amino acid residues, BIA 8-176, SAM, and Mg^{2+} for each monomer, as well as 554 water molecules. In addition, three 2,3-butanediol molecules and one MES molecule were modeled in the solvent region, between the two monomers. The last seven of eight residues in the C-terminal region are disordered and were not built in the crystallographic model, similarly to the crystal structures reported so far (Protein Data Bank codes 1VID, 1JR4, and 1H1D).

The structure is generally well defined within the electron density map, showing relatively low temperature factors (average B factor of 17 $Å^2$ for all protein atoms). In particular, the conformation of the inhibitor could be driven directly from initial maps. All protein residues lie within favored or allowed regions of the Ramachandran plot, except for Tyr68, which is an outlier, as also reported for previous S-COMT crystal structures (Vidgren et al., 1994; Bonifácio et al., 2002). The three-dimensional structure of S-COMT is a mixed α/β fold (Fig. 8), typical of methyltransferase enzymes, and the catalytic binding site is similar to previously determined structures (Vidgren et al., 1994; Vidgren and Ovaska, 1997; Bonifacio et al., 2002). The superposition of C_α atoms of S-COMT structure (residues 4–214) in complex with BIA 8-176 and with the inhibitors 3,5-dinitrocatechol (Protein Data Bank code 1VID), BIA 3-335 (Protein Data Bank code 1H1D), and bisubstrate (Protein Data Bank code 1JR4) shows an average RMSd between 0.31 and 0.37 for chain A and between 0.40 and 0.44 Å for chain B, whereas the RMSd between the two monomers of S-COMT/BIA8-176 is 0.27 Å.

COMT-BIA 8-176 Interactions. This is the first reported structure of S-COMT complexed with an inhibitor having a bulky substituent group in the position adjacent (*ortho*) to the nitro group. Three previously published complex structures (Vidgren et al., 1994; Lerner et al., 2001; Bonifácio et al., 2002) comprise inhibitors that carry different substituents at the *meta* position in relation to the nitro group (or the *N*-substituted dihydroxybenzamide moiety, in the case of the bisubstrate inhibitor) (Fig. 1).

It is noteworthy that the nitrocatechol moiety binds to the catalytic pocket in the *ortho* configuration, as in all other cocrystallized complexes, despite the modification of the attachment point of the side-chain substituent, relative to the nitro group. This binding mode positions the *ortho*-hydroxyl oxygen close to the methylsulfonium of SAM, whereas the benzoyl side chain is facing the edge of the catalytic pocket flanked by Trp143 and Met40. Another consequence attributable to the substitution pattern of the *ortho*-nitrated inhibitor is the out-of-the-plane torsions of the aryl nitro group and the carbonyl function of the benzoyl substituent. As

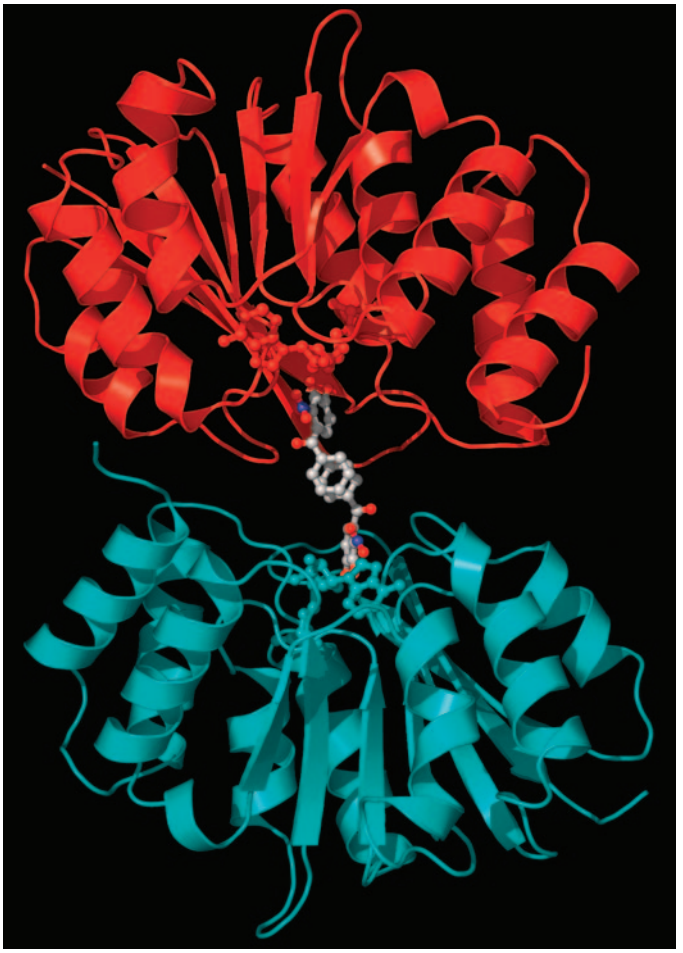

Fig. 8. Representation of the crystallographic dimer of S-COMT/SAM/BIA 8-176 complex. Monomer A is colored in cyan and monomer B in red. The cofactor SAM and the inhibitor BIA 8-176 are represented in ball and sticks mode. The inhibitor molecule is colored by element type (carbon, white; oxygen, red; nitrogen, blue). The inhibitor molecules from the two protein complexes are in straight contact with each other.

discussed above, these local distortions are also observed in our docking simulations and are probably due to the presence of intramolecular steric constraints within the inhibitor molecule and not imputable to intermolecular constraints imposed by the protein.

The inhibitor molecules from the two symmetric complexes are located on the dimer interface, in straight contact with each other (Fig. 9). In fact, the two phenyl rings, from the two BIA 8-176 molecules are very close to each other (with distances between proximal carbon atoms ranging from 3.5 to 4.4 Å) and are positioned in approximately parallel orientation. The Π stacking of the two aromatic rings helps preventing the exposure of the hydrophobic side chains of the inhibitors to the solvent and therefore may contribute to stabilizing the formation of crystals in the current space group. In addition, few van der Waals interactions are observed between the benzoyl substituent and protein residues, some of those, involving inhibitor and protein atoms from different monomers.

Molecular Modeling Analysis of the Crystallographic Complex. The electron density map corresponding to the ligand molecule in the complex reveals BIA 8-176 bound to the catalytic pocket in the *ortho* configuration. This structure is consistent with the preferred site of *O*-methylation by COMT as observed experimentally (Fig. 4) and is also predicted by molecular modeling calculations. However, the docking results also indicate that, for this particular configuration of the nitrocatechol pharmacophore, distinct families of bound conformations of BIA 8-176 may occur, presenting nearly degenerate interaction energies (Figs. 5C and 6). It is noteworthy that one of those docked conformations (Fig. 5C, solution #13) is virtually identical to that observed in the crystallographic structure, where the RMSd (ligand heavy atoms) between the two structures is only 0.3 Å. This is likely to stimulate curiosity as to why this particular conformation should be preferably stabilized in the crystal form of the complex, despite the fact that an ensemble of energetically equivalent bound conformations could, in theory, coexist in solution.

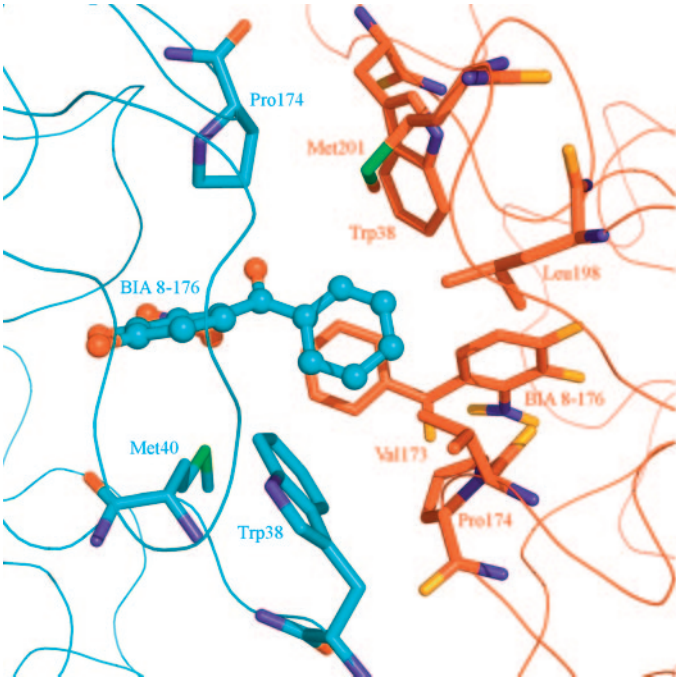

Fig. 9. Close-up view of ligand interactions. Residues located within 5.0 Å distance from the benzoyl substituent of BIA 8-176 (monomer A) are drawn in sticks. Carbon atoms from monomer A residues are colored in cyan and those from monomer B are depicted in red. Nitrogen and sulfur atoms are colored in blue and green, respectively. Oxygen atoms are shown in red for chain A residues and in orange for chain B residues. Besides the Π-staking interaction between the inhibitor molecules, other intra- and intermolecular hydrophobic contacts involving the BIA 8-176 substituent group and protein residues are present in the crystal structure.

The docking simulations described thus far were performed with the monomeric form of the enzyme, which is thought to be the physiologically active form. However, the crystal form of the complex, as obtained, reveals a protein dimer in the crystallographic asymmetric unit with intermonomer contacts in the region of the ligand-binding pocket. As described above, the benzoyl moiety of BIA 8-176 also establishes extended van der Waals contacts with atoms of the partner complex. Could such additional intermonomer interactions preferentially stabilize one particular conformation of the inhibitor? To test this hypothesis, we re-evaluated the docking simulations and the hydrophatic energy calculations using the crystallographic structure of the COMT dimer. Because the current docking algorithm cannot dock two ligand molecules to a protein dimer simultaneously and symmetrically, a specially modified procedure had to be employed. Each of the 40 docked structures of COMT/BIA 8-176 complex obtained from the previous docking simulations (using one COMT monomer) was duplicated and transformed using the same symmetry operations that relate the two polypeptide chains in the crystallographic dimer. In this way, 40 hypothetical complexes of COMT dimer with two symmetrically docked inhibitor molecules were quickly generated. As expected, some of the docked conformations presented steric conflicts with the second polypeptide chain or ligand molecule, because those atoms were not present during the initial docking run. Therefore, all complexes were fully optimized by energy minimization to allow the docked poses to readjust to their new chemical environment in the dimer. Finally, the hydrophatic interactions of each refined ligand with the two protein monomers and second inhibitor molecule were calculated. Figure 10 plots these values (filled symbols) and compares them to those obtained before, with one COMT monomer (unfilled markings). The RMSd values refer to differences between docked conformations and the crystallographic coordinates of BIA 8-176 (in monomer A).

It is noteworthy that every docked conformation becomes further stabilized in the dimeric form of the complex compared with those in the monomeric form. Such additional stabilization is due to the formation of favorable contacts between the benzoyl side chain of the inhibitor and the other protein monomer or, in some poses, also the side chain of the second ligand molecule. Most surprisingly however, the energy degeneracy of the different docked conformations in the *ortho* configuration (Fig. 6, circles) (HINT scores ~1540 ± 70) is apparently "lifted" when the dimer form of the complex is considered. In this situation, docked solution #13′ (obtained from structure 13, in the monomeric complex) stands out as the most stable bound conformation, with a HINT score of approximately 300 units higher than any other solution. To establish a common ground of comparison between the predicted (docked solution #13′) and crystallographic conforma-

tions, the crystal structure of the complex was also refined (both monomeric and dimeric forms) by energy minimization (Fig. 10, X markings). The predicted and crystallographic structures of the bound inhibitor are remarkably identical, with RMSd = 0.03 Å (ligand heavy atoms), and have identical HINT scores.

Finally, the nature of the stabilizing interactions, involving BIA 8-176 at the interface of the dimeric complex, was evaluated in detail by identifying the individual contributions to the hydrophatic potentials. Figure 11 represents isopotential contour maps representing the stabilizing hydrophobic interactions of BIA 8-176 (ball and sticks representation) with the surrounding atoms in the crystallographic complex (for simplicity, the polar interactions of the catechol moiety are not represented). The interactions with residues of monomer A (cyan), represented as green surfaces, are mostly accounted for by the nitrocatechol moiety and the side chains of residues flanking the active site. In a physiological complex involving one single COMT monomer, the hydrophobic phenyl ring of the inhibitor side chain would extend into the solvent, unable to make relevant contacts with the protein. The binding affinity is therefore primarily ensured by the interactions of the nitrocatechol moiety and benefits from the lack of major steric clashes.

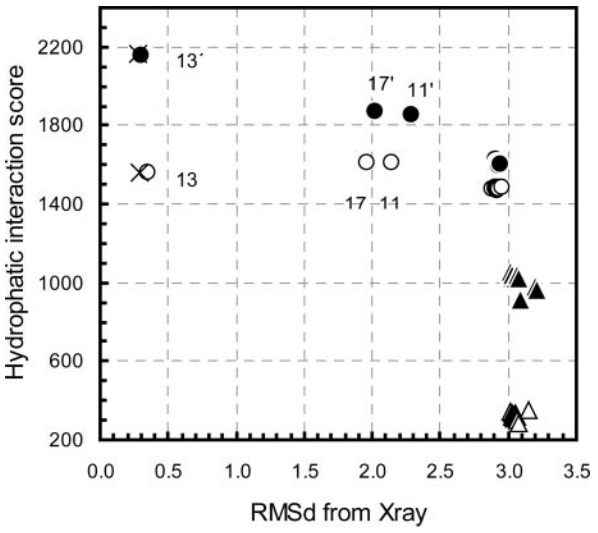

Fig. 10. Comparison of HINT interaction scores of BIA 8-176 docked to one monomer (white markings) or to the crystallographic dimer of COMT (black symbols). Circles represent molecules docked in *ortho* configuration, whereas *meta* poses are represented as triangles. The abscissa represents the RMSd between the atomic coordinates of each docked structure and those in the crystallographic complex. Higher HINT scores indicate more stable complexes.

The formation of the crystallographic dimer, however, provides an opportunity for establishing additional stabilizing contacts that may shield the hydrophobic side chain of the inhibitor from the solvent (contour surface in magenta). That is to say, the hydrophobic residues Trp38, Val173, Pro174, Leu198, and Met201 of monomer B (Fig. 11, red) and the side chain of the second molecule of the inhibitor (gold) form a hydrophobic pocket, where the benzoyl moiety fits in and establishes energetically favorable interactions. Such interactions constitute the basis for the additional stabilization of this particular bound conformation.

Discussion

In the present study, the interactions of COMT with two related nitrocatecholic inhibitors, which have benzoyl side-chain substituents at the *ortho* and *meta* position relative to the aryl nitro group, were compared. The two inhibitors are slowly metabolized by COMT in vitro, each producing different levels of mono-*O*-methyl-ether conjugates. The regioselectivity of *O*-methylation is shown to be greatly affected by the substitution pattern of the two molecules. We have studied the molecular interactions of the two molecules within the catalytic site and the chemical susceptibility of each of the hydroxyl groups to undergo *O*-methylation by means of docking simulations and molecular orbital calculations. These theoretical results provide a plausible interpretation of

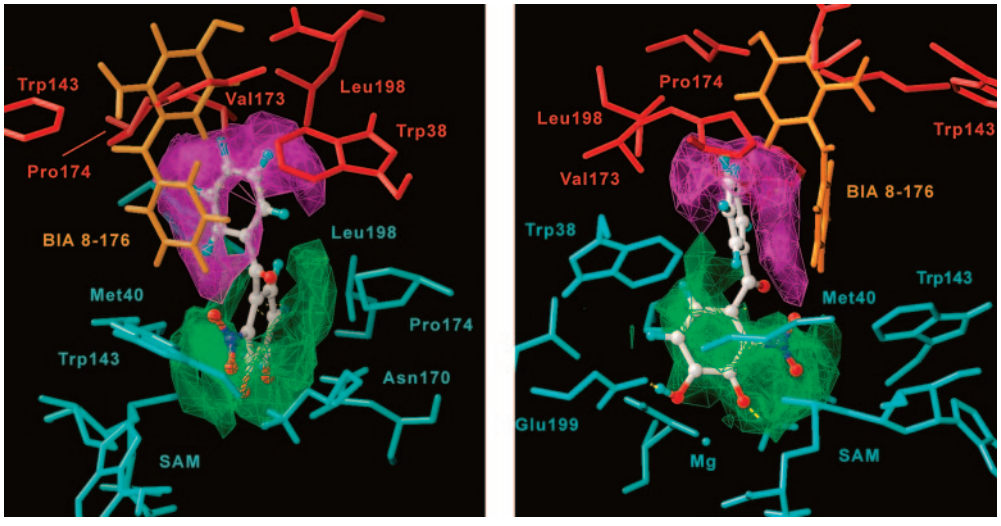

Fig. 11. HINT isopotential contour maps, representing favorable hydrophobic interactions between COMT and BIA 8-176, in the dimeric crystallographic complex. Left and right panels represent approximately perpendicular views of the same structure. The inhibitor molecule is represented in ball and sticks and colored by element type (carbon, white; hydrogen, cyan; oxygen, red; nitrogen, blue). The inhibitor is complexed at the active site of the crystallographic monomer A of COMT (cyan) and interacts with monomer B residues (red), at the interface of the dimer, and with a second inhibitor molecule (orange), bound to monomer B. Green isopotential contour surfaces indicate regions of stabilizing hydrophobic interactions exclusively between BIA 8-176 and protein chain A (intracomplex). Surface in magenta represents the interactions of BIA 8-176 with the second complex structure within the crystal (intercomplex).

the observed regioselectivities and enable the identification of the major structural and chemical factors that determine the preferred methylation sites. Finally, the X-ray structure of the complex of COMT with SAM and BIA 8-176 is herein disclosed, and some structural and dynamic aspects of this complex are analyzed and discussed.

The analysis of docking calculations indicates that the geometry of the enzyme-inhibitor complex is primarily determined by the nitrocatechol moiety. Although this molecular fragment may potentially adopt either *ortho* or *meta* configurations within the catalytic pocket, our calculations indicate that the *meta* poses should be energetically penalized as a result of sterically conflicting interactions between the nitro group and the side chain of Leu198 and repulsive electrostatic forces with the negatively charged Glu199. Conversely, the nitro group can be easily accommodated at the opposite side of the catalytic pocket, in the *ortho* configuration, where it establishes favorable van der Waals contacts with Trp143. The results suggest that interactions involving the benzoyl side chain may also affect the energetic balance between *ortho* and *meta* poses. Their contribution should however, be considerably less determinant than those of the nitrocatechol moiety. The simultaneous contributions of the nitro and benzoyl substituents within the structures of the two regioisomers, may result in the potentiation or the attenuation of the energy gaps between the *ortho* or *meta* complex configurations. In the case of BIA 8-176, where the benzoyl occupies the *ortho* position relative to the nitro group, the effects of the two substituents are additive with respect to the influence they exercise on determining the binding geometry. Therefore, this complex presents a greater binding regioselectivity with the *ortho* configuration greatly favored in relation to the "*meta* complex". The *meta*-nitrated inhibitor BIA 3-228, on the other hand, shows a distinct behavior. Even though the *ortho* bound configuration is still energetically favorable, the effects of the two substituents on the binding geometry are partially self-compensatory, and the energy difference between *ortho* and *meta* poses is relatively attenuated. The regioselectivity of binding predicted for this complex, is therefore less pronounced than that expected between COMT and BIA 8-176.

Although the relative position of attachment of the benzoyl group to the catechol ring may have a limited influence on the geometry of binding of the inhibitor within the catalytic site, it is suggested that it will have a profound impact on the chemical reactivity of the two hydroxyl groups. Electron-withdrawing substituents on the catechol ring contribute to the delocalization of the excess electron density, away from the reactive ionized catecholate oxygen. In this way, such groups lower the nucleophilicity of the hydroxyls and hence reduce their propensity to react with the electron-deficient methyl group from SAM. It is demonstrated that the relative positions of the two substituents strongly affect the nucleophilicity balance between the two hydroxyl groups. In the *meta*-nitrated molecule BIA 3-228, the benzoyl and the nitro substituents exert a combined inductive effect that is maximal on the catecholate hydroxyl oxygen found *ortho* to the nitro (and *para* to the benzoyl substituent). Therefore, the reactivity of this hydroxyl is strongly diminished, compared with that of the unsubstituted catechol (Fig. 7). On the contrary, the second hydroxyl function, which is *meta* to both substituents, is the least perturbed and therefore should be more readily methylated, should the appropriate orientation within the catalytic site be allowed. The *ortho*-nitrated inhibitor BIA 8-176 bears two adjacent substituent groups on the catechol ring (Fig. 2). This substitution pattern allows the benzoyl substituent to exert a maximal delocalizing effect on the catechol hydroxyl in the *meta* position relative to nitro (*para* position relative to the benzoyl group), whereas the other catechol hydroxyl is primarily affected by the electron-withdrawing nitro group in the *ortho* position. As a result, the reactivity indices of these two catechol hydroxyls approach each other's values, midway between the reactivities of the *ortho* and *meta* hydroxyls of BIA 3-228 (Fig. 7).

The observed regioselectivity of the enzymatic *O*-methylation can be qualitatively interpreted by the combined analysis of the docking results and the calculated chemical reactivity indices. The calculated chemical reactivities of the "activated" hydroxyl oxygens, within the active site, indicate that the complexes formed in *ortho* configuration are generally less reactive than those complexes formed in the alternative orientation. Therefore, the highly selective methylation of BIA 8-176 at the *ortho* hydroxyl position should be mostly determined by the selective formation of an enzyme-inhibitor complex in ortho configuration, as suggested by our docking results. In this case, the intrinsic reactivities of the two catechol hydroxyls are both moderately hindered by the catechol substituents and nearly degenerated; therefore, reactivity should not be a dominant factor to the observed regioselectivity.

Conversely, the ratio of *ortho*- and *meta*-*O*-methyl metabolites formed from BIA 3-228 is determined by a balance between two opposing terms. Although the current docking results suggest that the formation of the Michaelis complex should occur predominantly in the *ortho* configuration, this would in fact lead to an essentially low-reactivity arrangement. On the other hand, those molecular collisions leading to *meta*-configuration complexes would bring the substantially more reactive *meta*-hydroxyl into an optimal geometry for methylation. As a result, the extent of *ortho*-*O*-methylation is reduced, whereas that of *meta*-methylation is enhanced compared with the corresponding relative *O*-methylation levels of BIA 8-176. Given a suitable balance between the two opposing trends, an inversion of the *O*-methylation regioselectivity may occur, as indeed was observed (Fig. 4).

The crystallographic structure of the ternary COMT/SAM/BIA 8-176 complex is disclosed and discussed herein. The highly resolved atomic coordinates clearly show the inhibitor BIA 8-176 adopting an *ortho* configuration within the catalytic pocket, indicating that this pose should correspond to the energetically most favorable docked configuration. This is in agreement with current theoretical data. However, neither the current crystallographic data nor any other known X-ray complexes would provide, per se, a structural model for the mechanism of *O*-methylation of nitrocatechol inhibitors, at the hydroxyl oxygen *meta* to the nitro group. Nevertheless, the pool of experimental and theoretical results, presented herein, indicate that the formation of alternative complex forms, which could give rise to *meta*-*O*-methylated conjugates (Fig. 4), should not be overlooked.

In addition, although the crystallographic conformation of the benzoyl side chain of BIA 8-176 may indeed represent the thermodynamically most stable conformation within the framework of the crystal, it is suggested that this particular

conformation could result from nonphysiological stabilizing interactions at the interface of the crystallographic dimer. Therefore, with regard to the orientation the benzoyl moiety, an ensemble of competing bound conformations would probably better represent a physiological picture of this complex. In conclusion, the crystallographic structure obtained, although elucidating and rich in structural information, may capture only partial aspects of the full complexity and dynamics of the molecular interactions and enzymatic *O*-methylation of this inhibitor by COMT. We show that the docking simulations and theoretical calculations may profitably complement crystallographic studies, which allows a wider exploration of the binding configuration space and reactivity profiles, thereby providing a more integrated interpretation of the experimental biochemical data.

In conclusion, the results herein described are relevant to understanding certain aspects of the pharmacokinetic profiles of this class of COMT inhibitors. It was shown that altering the position of the benzoyl substituent from the *meta* to *ortho* position, relative to the nitro group, as in the case of BIA 3-228 and BIA 8-176, produces a profound effect on the in vitro regioselectivity of the *O*-methylation catalyzed by COMT. Moreover, a plausible interpretation of those effects at the molecular level was only possible by a proper combination of experimental and theoretical approaches, which provide complementary information. Indeed, it is hypothesized that the differences in enzymatic regioselectivity observed with the two isomeric compounds are attributed to a delicate balance between selective preorientations of the inhibitors within the catalytic site and the relative chemical reactivity of each methylation site. The present case study is limited to the two compounds BIA 3-228 and BIA 8-176, but the methodological approach and rationales herein used may serve as a basis to study other COMT inhibitors, possessing different catechol substituents other than the nitro and benzoyl groups.

References

Bäckström R, Honkanen E, Pippuri A, Kairisalo P, Pystynen J, Heinola K, Nissinen E, Linden IB, Männistö PT, and Kaakkola S (1989) Synthesis of some novel potent and selective catechol-*O*-methyltransferase inhibitors. *J Med Chem* **32:**841–846.

Bonifácio MJ, Archer M, Rodrigues ML, Matias PM, Learmonth DA, Carrondo MA, and Soares-Da-Silva P (2002) Kinetics and crystal structure of catechol-*O*-methyltransferase complex with co-substrate and a novel inhibitor with potential therapeutic application. *Mol Pharmacol* **62:**795–805.

Bonifacio MJ, Vieira-Coelho MA, and Soares-da-Silva P (2003) Kinetic inhibitory profile of BIA 3–202, a novel fast tight-binding, reversible and competitive catechol-*O*-methyltransferase inhibitor. *Eur J Pharmacol* **460:**163–170.

Bonifati V and Meco G (1999) New, selective catechol-*O*-methyltransferase inhibitors as therapeutic agents in Parkinson's disease. *Pharmacol Ther* **81:**1–36.

Borgulya J, Bruderer H, Bernauer K, Zurcher G, and Da Prada M (1989) Catechol-*O*-methyltransferase—inhibiting pyrocatechol derivatives: synthesis and structure-activity studies. *Helv Chim Acta* **72:**952–968.

Chen D, Wang CY, Lambert JD, Ai N, Welsh WJ, and Yang CS (2005) Inhibition of human liver catechol-*O*-methyltransferase by tea catechins and their metabolites: structure-activity relationship and molecular-modeling studies. *Biochem Pharmacol* **69:**1523–1531.

Creveling CR, Morris N, Shimizu H, Ong HH, and Daly J (1972) Catechol-*O*-methyltransferase. IV. Factors affecting *m*- and *p*-methylation of substituted catechols. *Mol Pharmacol* **8:**398–409.

Da Prada M, Borgulya J, Napolitano A, and Zurcher G (1994) Improved therapy of Parkinson's disease with tolcapone, a central and peripheral COMT inhibitor with an S-adenosyl-L-methionine-sparing effect. *Clin Neuropharmacol* **17:**S26–S37.

Dingemanse J, Jorga K, Zürcher G, Fotteler B, Sedek G, Nielsen T, and van Brummelen P (1996) Multiple-dose clinical pharmacology of the catechol-*O*-methyltransferase inhibitor tolcapone in elderly subjects. *Eur J Clin Pharmacol* **50:**47–55.

Fukui K, Yonezawa T, and Nagata C (1954) Theory of substitution in conjugated molecules. *Bull Chem Soc Japan* **27:**423–427.

Fukui K, Yonezawa T, and Nagata C (1957) Interrelations of quantum-mechanical quantities concerning chemical reactivity of conjugated molecules. *J Chem Phys* **26:**831–841.

Halgren TA (1996) Merck molecular force field. I. Basis, form, scope, parameterization and performance of MMFF94. *J Comput Chem* **17:**490–519.

Halgren TA (1999) MMFF VII. Characterization of MMFF94, MMFF94s and other widely available force fields for conformational energies and for intermolecular-interaction energies and geometries. *J Comput Chem* **20:**730–748.

Jones G, Willett P, and Glen RC (1995a) A genetic algorithm for flexible molecular overlay and pharmacophore elucidation. *J Comput Aided Mol Des* **9:**532–549.

Jones G, Willett P, and Glen RC (1995b) Molecular recognition of receptor sites using a genetic algorithm with a description of desolvation. *J Mol Biol* **245:**43–53.

Jones G, Willett P, Glen RC, Leach AR, and Taylor R (1997) Development and validation of a genetic algorithm for flexible docking. *J Mol Biol* **267:**727–748.

Kahn K and Bruice TC (2000) Transition-state and ground-state structures and their interaction with the active-site residues in catechol-*O*-methyl transferase. *J Am Chem Soc* **122:**46–51.

Karelson M and Lobanov VS (1996) Quantum-chemical descriptors in QSAR/QSPR studies. *Chem Rev* **96:**1027–1043.

Kellogg GE, Joshi GS, and Abraham DJ (1992) New tools for modeling and understanding hydrophobicity and hydrophobic interactions. *Med Chem Rev* **1:**444–453.

Kuhn B and Kollman PA (2000) QM-FE and molecular dynamics calculations on catechol-*O*-methyltransferase: free energy of activation in the enzyme and in aqueous solution and regioselectivity of the enzyme-catalyzed reaction. *J Am Chem Soc* **122:**2586–2596.

Lau EY and Bruice TC (1998) Importance of correlated motions in forming highly reactive near attack conformations in catechol-*O*-methyltransferase. *J Am Chem Soc* **120:**12387–12394.

Lautala P, Ulmanen I, and Taskinen J (2001) Molecular mechanisms controlling the rate and specificity of catechol-*O*-methylation by human soluble catechol-*O*-methyltransferase. *Mol Pharmacol* **59:**393–402.

Learmonth DA, Bonifacio MJ, and Soares-da-Silva P (2005) Synthesis and biological evaluation of a novel series of "*ortho*-nitrated" inhibitors of catechol-*O*-methyltransferase. *J Med Chem* **48:**8070–8078.

Learmonth DA and Freitas AP (2002) Chemical synthesis and characterization of conjugates of a novel catechol-*O*-methyltransferase inhibitor. *Bioconjug Chem* **13:**1112–1118.

Learmonth DA, Palma PN, Vieira-Coelho MA, and Soares-da-Silva P (2004) Synthesis, biological evaluation and molecular modeling studies of a novel, peripherally selective inhibitor of catechol-*O*-methyltransferase. *J Med Chem* **47:**6207–6217.

Learmonth DA, Vieira-Coelho MA, Benes J, Alves PC, Borges N, Freitas AP, and Soares-da-Silva P (2002) Synthesis of 1-(3,4-dihydroxy-5-nitrophenyl)-2-phenylethanone and derivatives as potent and long-acting peripheral inhibitors of catechol-*O*-methyltransferase. *J Med Chem* **45:**685–695.

Lerner C, Ruf A, Gramlich V, Masjost B, Zürcher G, Jakob-Roetne R, Borroni E, and Diederich F (2001) X-ray crystal structure of a bisubstrate inhibitor bound to enzyme catechol-*O*-methyltransferase: a dramatic effect of inhibitor preorganization on a binding affinity. *Angew Chem Int Ed* **40:**4040–4042.

Lotta T, Vidgren J, Tilgmann C, Ulmanen I, Melen K, Julkunen I, and Taskinen J (1995) Kinetics of human soluble and membrane-bound catechol-*O*-methyltransferase: a revised mechanism and description of the thermolabile variant of the enzyme. *Biochemistry* **34:**4202–4210.

Männistö PT and Kaakkola S (1989) New selective COMT inhibitors: useful adjuncts for Parkinson's disease? *Trends Pharmacol Sci* **10:**54–56.

Männistö PT and Kaakkola S (1990) Rationale for selective COMT inhibitors as adjuncts in the drug treatment of Parkinson's disease. *Pharmacol Toxicol* **66:**317–323.

Nissink JWM, Murray C, Hartshorn M, Verdonk ML, Cole JC, and Taylor R (2002) A new test set for validating predictions of protein-ligand interaction. *Proteins* **49:**457–471.

Palma PN, Bonifacio MJ, Loureiro AI, Wright LC, Learmonth DA, and Soares-Da-Silva P (2003) Molecular modeling and metabolic studies of the interaction of catechol-*O*-methyltransferase and a new nitrocatechol inhibitor. *Drug Metab Dispos* **31:**250–258.

Rodrigues ML, Bonifacio MJ, Soares-da-Silva P, Carrondo MA, and Archer M (2005) Crystallisation and preliminary X-ray diffraction studies of a catechol-*O*-methyltransferase/inhibitor complex. *Acta Crystallogr Sec D* **61:**118–120.

Roussel A and Cambilau C (1989) Turbo-Frodo, in *Silicon Graphics Geometry Partners Directory*, pp 77–78, Silicon Graphics, Mountain View, CA.

Sipila J and Taskinen J (2004) CoMFA modeling of human catechol-*O*-methyltransferase enzyme kinetics. *J Chem Inf Comput Sci* **44:**97–104.

Thakker DR, Boehlert C, Kirk KL, Antkowiak R, and Creveling CR (1986) Regioselectivity of catechol-*O*-methyltransferase. The effect of pH on the site of *O*-methylation of fluorinated norepinephrines. *J Biol Chem* **261:**178–184.

Verdonk ML, Cole JC, Hartshorn MJ, Murray CW, and Taylor RD (2003) Improved protein-ligand docking using GOLD. *Proteins* **52:**609–623.

Vidgren J and Ovaska M (1997) Structural aspects in the inhibitor design of catechol-*O*-methyltransferase, in *Structure-Based Drug Design* (Veerapandian P ed), Marcel Dekker, Inc., New York.

Vidgren J, Svensson LA, and Liljas A (1994) Crystal structure of catechol-*O*-methyltransferase. *Nature (Lond)* **368:**354–358.

Zheng YJ and Bruice TC (1997) A theoretical examination of the factors controlling the catalytic efficiency of a transmethylation enzyme—catechol-*O*-methyltransferase. *J Am Chem Soc* **119:**8137–8145.

Address correspondence to: P. Nuno Palma, Department of Research and Development, Bial., À. Av. da Siderurgia Nacional, 4745–457 S. Mamede do Coronado, Trofa, Portugal. E-mail: nuno.palma@bial.com